QUANTITATIVE ANALYSIS OF THE INTRAMEDULLARY ARTERIAL SUPPLY OF THE FELINE TIBIA: IS THERE A CAUSAL RELATIONSHIP TO DELAYED AND NONUNION FRACTURE HEALING?

By

DANIELLE R. DUGAT, DVM

Bachelor of Science in Animal Science

California State Polytechnic University, Pomona

Pomona, California

2003

Submitted to the Faculty of the
Graduate College of the
Oklahoma State University
in partial fulfillment of
the requirements for
the Degree of
MASTER OF SCIENCE
May, 2011

QUANTITATIVE ANALYSIS OF THE INTRAMEDULLARY ARTERIAL SUPPLY OF THE FELINE TIBIA; IS THERE A CAUSAL RELATIONSHIP TO DELAYED AND NONUNION FRACTURE HEALING?

Thesis Approved:

Dr. Mark C. Rochat

Thesis Adviser

Dr. Jerry W. Ritchey

Dr. Kenneth E. Bartels

Dr. Mark E. Payton

Dean of the Graduate College

ACKNOWLEDGMENTS

We would like to thank Alastair Watson, Ph.D. and Damon Chandler, Ph.D. for their technical support in using the Spalteholz technique and ImageJ morphometric software program.

We would also like to thank Roger Panciera, DVM, Ph.D., DACVP for his technical advice on photographing specimens.

Lastly, we owe appreciation to Susan Little, DVM, Ph.D., DEVPC, Misti West Spatz, Carole Muchmore, Ph.D., and Eileen Johnson, DVM, MS, Ph.D. for allowing use of their dissecting microscopes and SpotSoftware® image program.

TABLE OF CONTENTS

LIST OF TABLES

Table Page

LIST OF FIGURES

Figure Page

CHAPTER I

INTRODUCTION

The tibia is the second most commonly fractured long bone in cats, with a reported incidence rate of 10-20% of all long bone fractures (1-4). Clinical observations suggest that tibial fractures in cats are prone to fracture healing complications, including development of delayed union and nonunion (1, 2, 5, 6). Delayed union is characterized by failure of a fracture to heal within the expected time; however, evidence of healing is observed. Alternately, nonunion is a condition characterized by cessation of fracture healing. Nolte *et al.* identified a 61.1% nonunion rate associated with tibial fractures in cats, most of which were identified as comminuted, diaphyseal fractures (2). Factors that have been postulated to result in delayed union or nonunion include a lack of adequate blood supply provided by extraosseous soft tissue, lack of stable fixation, large fracture gaps, and interposition of soft tissue between the ends of the fractured bone (1, 2, 7-9). Thus, the surgeon's goals in fracture repair should include rigid fixation, anatomic reduction, and preservation of blood supply (7, 9, 10).

The tibia of all mammalian species is prone to complications associated with fracture healing because of the limited soft tissue overlying the bone along its entire medial surface. This lack of soft tissue coverage makes these fractures more susceptible to open fracture, stripping of the periosteum, and delayed revascularization of the bone (2, 6, 11). Periosteal stripping has been shown to reduce cortical blood flow initially by 20% in a sheep model (12), and fracture healing, in its early stage, is dependent on the periosteal blood supply. The lack of intramedullary arterial

supply early in the healing process, combined with a paucity of extraosseous blood supply in the form of soft tissue and periosteal vascularization, contributes to delays in fracture healing (2, 6, 9).

The most common sites for nonunion fracture healing in dogs are the radius and ulna, femur, and humerus (2, 7, 11, 13, 14). Although marginal vascular supply to the tibia has been implicated as a significant cause of delayed union and nonunion fracture healing complications in cats, dogs seemingly do not experience the same degree of delayed union and nonunion. Therefore, dogs can provide a model for comparison to determine if the intramedullary arterial supply of the feline tibia is adequate for fracture healing or whether it should be considered as a potential factor in delayed union and nonunion feline tibial fractures.

Although a poor arterial supply to the tibia has been anecdotally reported as a significant risk factor for delayed union and nonunion complications (2, 7-9), there exists no detailed description of the intramedullary arterial anatomy of the feline tibia. One objective of this study was to provide an accurate delineation of the intramedullary arterial supply of the adult feline tibia. Additionally, the study aimed to determine if the arterial supply is significantly different from that of adult dogs, suggesting a causal link to delays in fracture healing. Our null hypothesis was that the intramedullary arterial density and the diameter of the nutrient artery in the adult feline tibia is the same when compared to an age and size matched dog.

CHAPTER II

REVIEW OF LITERATURE

TIBIAL FRACTURES

Veterinary literature has provided incidence rates for feline tibial fractures; the tibia is the second most commonly fractured long bone in cats. Harari summarizes some of the findings documented in veterinary literature (1), which are provided below (Table 1).

Table 1. Percentage of Long Bone Fractures in Cats

Bone	Hill (1977)	Knecht (1978)	Schrader (1994)	Smith (1994)
Humerus	5%	8%	5%	---
Radius/ulna	3%	5%	7%	7%
Femur	38%	20%	30%	30%
Tibia/fibula	**10%**	**14%**	**8%**	**8%**

Tibial fractures have been shown to frequently occur in the tibial diaphysis, where the triangularly shaped bone is smallest in diameter (9). Boone *et al.* identified that in 195 fractures associated with the tibia in cats and dogs, 39 (20%) involved the proximal diaphysis, 126 (64.6%) involved the mid-diaphysis, and 30 (15.4%) involved the distal diaphysis (5). Likewise, Richardson *et al.* identified the highest prevalence of tibial fractures in cats to be in the mid-diaphyseal section of bone (n = 50/80), a rate of 62% (6). This data alone does not correlate with an increased incidence of delayed union and nonunion fracture healing in feline tibial fractures as many reported incidence rates include canine populations as well. It is important to note that the

relative lack of extraosseous soft tissue primarily on the medial surface of the tibia renders fractures having a high risk of comminution and/or becoming open fractures, thus increasing the susceptibility of fracture healing complications.

BLOOD SUPPLY – NORMAL LONG BONE

In order to determine whether or not a difference in the tibial intramedullary arterial supply between dogs and cats exists, it is important to understand the normal blood supply to a long bone. Adequate blood supply is necessary for any physiologic process to occur in a normal functioning bone (10). Normal circulation to long bones consists of an afferent supply from three sources: the proper nutrient artery, proximal and distal metaphyseal arteries, and periosteal arteries (10, 15, 16).

The proper nutrient artery arises from a principal artery (i.e. caudal tibial artery, a branch of the popliteal artery) and courses through the extraosseous fascia until it penetrates the bony cortex along a major fascial attachment within the proximal third of the tibial diaphysis. The nutrient artery travels through the cortex to the medullary cavity, where it divides into ascending and descending branches. These branches further divide into arterioles, which radiate from the nutrient artery. The arterioles enter the cortex, thus supplying the inner two-thirds of cortical bone. Approximately 30% of the blood flow is directed to the medullary cavity while the remaining 70% supplies the cortices (16).

Metaphyseal arteries are branching arteries from neighboring systemic vessels. In healthy bone, these vessels do not provide a substantial contribution to the afferent vascular system. Instead, these vessels serve as an efferent supply from the metaphysis as their terminal branches anastamose with arterioles of the proper nutrient artery at the ends of the medullary cavity (16). With damage to the proper nutrient artery, the metaphyseal arteries can alternately hypertrophy and assume cortical blood supply until the intramedullary arterial supply is re-established.

Periosteal arterial supply is well developed in the immature animal. The blood supply is oriented longitudinally within the periosteum. The enhanced blood supply in the young patient is important in allowing growth of long bones. As the patient matures the periosteal arterioles atrophy and contact bony surfaces at ligamentous or fascial attachments (17). It is at these attachments that the periosteal arteries supply the outer one-third of the bony cortices. Terminal branches of the periosteal arterioles anastamose with the medullary arterioles within the cortices.

Hulse *et al.* state that under normal conditions, the direction of blood flow through the diaphysis is centrifugal, from the medullary canal to periosteum (10). Medullary pressure created by this pattern of blood flow likely restricts periosteal blood flow from supplying any more than the outer one-third of the cortex. Remedios adds that the drainage of blood via the efferent vascular system occurs primarily in a centripetal direction (16). Likewise, Rhinelander and Trueta state that blood flow following a fracture is altered from its normal centrifugal orientation to a centripetal orientation (17, 18).

In both adult and immature animals, the cortex and medullary cavity are drained separately. Within the medullary cavity, the venous branches empty into sinusoids, which pool into a central medullary sinus. Accompanying veins and the nutrient vein penetrate the cortex to return blood to the venous circulation. Before proceeding into systemic circulation, blood from the cortex flows toward the periosteal surface and empties into venules that join periosteal veins (16).

BLOOD SUPPLY – FRACTURED LONG BONE

With long bone fractures, medullary circulation is disrupted. Existing vasculature enhances to aid in supplying the injured bone segment. Additionally, a transient extraosseous vascular supply develops within soft tissues to nourish the early periosteal callus. As bone healing progresses, medullary blood supply is re-established. Ultimately, the extraosseous circulation diminishes and normal medullary centrifugal flow dominates.

FRACTURE HEALING

Healing is a process of restoring tissue function. Healing and repair of fractured bone involves multiple events that can be loosely divided into three main phases: inflammation, repair, and remodeling (16). Events within a given phase often overlap with those of the subsequent phase.

The inflammatory phase of bone healing begins immediately after a fracture occurs, involving vascular and cellular responses to injury. Bone, vascular, and soft tissue damage stimulate the release of inflammatory (vasoactive) mediators, exudation of plasma, and migration of inflammatory cells. The result is swelling, erythema, pain, and impaired tissue function. Vasoactive mediators, including serotonin, histamine, and thromboxane $A_{2,}$ are responsible for vasodilation and the increased permeability of local vasculature (20). Subsequently, blood leaks into the injured tissue (i.e. fracture site), forming a hematoma. The organized hematoma contains fibrin and platelets that bind to collagen to form a clot. The clot remains within the surrounding periosteum to occupy the injured site and form an early scaffold for migration of reparative cells. Platelets release vasoactive mediators secondary to activation of the coagulation cascade and growth factors (eg. transforming growth factor-β, fibroblast growth factor, platelet derived growth factor). Blood vessel endothelial cells release platelet derived growth factor, nerve tissue produces fibroblast growth factor, macrophages produce interleukin-1, and fibroblasts secrete platelet derived growth factor and TGF-β. These growth factors collectively stimulate the proliferation of repair tissue in the second phase of healing (21).

In addition to hematoma formation, the inflammatory phase is initiated coincidentally by the stimulus to remove devitalized osteocytes within the adjacent fractured bone (19). The first cell to migrate to the site of injury is the polymorphonuclear leukocyte. Soon after, monocytes and T-lymphocytes arrive at the site of injury (20). Mast cells and macrophages (derived from monocytes) are also present within the local environment. Each of these inflammatory cells can

release cytokines to stimulate vascular invasion of tissue and migration of mesenchymal cells, which can become osteoprogenitor cells. Blood vessels surrounding the site of injury proliferate during the inflammatory phase to form new capillaries that extend into the fracture site, restoring the vascular supply to the injured tissue needed for the repair phase.

The repair phase involves replacement of necrotic and damaged tissue by new cells and matrix. This phase occurs in the presence of undifferentiated mesenchymal cells that migrate to the injured site with inflammation (20). The mesenchymal cells have the capacity to form new bone, cartilage, fibrous tissue, or blood vessels. After entering into the injured tissue, the mesenchymal cells proliferate and synthesize new matrix (callus). The matrix formation is initially high in collagen concentration; however, the biologic environment determines what specific function (chondrocytes, osteoblasts, fibroblasts or other cell types) a given mesenchymal cell will assume (20). Concentrations of growth factor, hormones, nutrients, local pH, and oxygen tension help to control matrix synthesis and differentiation. The callus functions to provide a scaffold within and surrounding the fracture site. It can be divided into a soft, fibrous callus and hard (bony) callus. The soft callus is primarily composed of cartilage and occupies the central region where oxygen tension is low. Hard callus is formed at the periphery where vascular supply is greater and therefore oxygen tension is higher. The hard callus forms initially by intramembranous bone formation.

The final phase is the remodeling phase. The remodeling process is a prolonged event because it involves reshaping and reorganizing reparative tissue by removal, replacement, and reorganization of the callus. Repair tissue is highly disorganized; remodeling allows the tissue to develop into a more structurally sound and biologically more functional tissue than the original tissue. As remodeling progresses, cell density and vascularity decrease, the unorganized matrix fibrils re-orient along the lines of stress, and new bone formation occurs (20). Simply, bone replaces cartilage via endochondral ossification, increasing the percentage of the hard callus and

fracture stability. In the late stages of remodeling, woven bone is replaced by lamellar bone and callus resorption occurs in areas where it is no longer needed.

Although the preceding discussion represents the “classical” description of bone healing, variations exist depending on the type of fracture environment that is present, both mechanical and biological. For example, repair of an unstable fracture, open fracture, or one with intramedullary fixation may disrupt the early fracture hematoma and thus delay the subsequent phases of healing. In addition, the extent of fracture stability and degree of fracture gap play a large role in determining the extent of the need for callus formation. New bone formation can occur via 1) a cartilage precursor (endochondral bone formation), 2) direct bone healing (bone formation without callus), or3) callus formation (intramembranous bone formation) (10, 20).

With direct bone healing, callus formation is not necessary as the fracture surfaces are in contact with one another and rigid stability is present. As a result, osteoblasts are capable of crossing the gap at the fracture site. Conversely, indirect bone healing involves the formation of a cartilaginous callus at the fracture site because of the presence of an unstable fracture and/or significant gaps between the ends of the fractured bone. A third and, perhaps, intermediate method of bone healing is intramembranous bone formation. Intramembranous bone formation is a type of direct bone healing that occurs when a small amount of strain is present at the fracture site. An example of this type of bone healing is bone being directly deposited on the bone fragments within a large fracture gap, such as the bone that can develop between comminuted segments of bone.

DELAYED AND NONUNION FRACTURE HEALING

In addition to identifying the normal blood supply and fracture healing of a long bone, it is important to understand factors that play a role in delayed union and nonunion fracture healing complications. Across species, delayed union can be defined as a fracture that has not healed

within a time expected. However, there is evidence of fracture healing present. Alternatively, nonunion is a condition in which all healing has ceased (2). Human orthopedic surgeons have not agreed on the length of time required for a tibial fracture to heal, but the United States Food and Drug Administration has defined nonunion as a fracture that has no radiographic evidence of progression toward healing for three consecutive months (22). Nonunions are further classified by their radiographic appearance as vascular (viable) or avascular (nonviable). Vascular nonunions have varying degrees of callus surrounding the bone, but a persistent radiolucent line at the fracture site. There is an adequate biologic environment, but a lack of sufficient fracture stability. Avascular nonunions have little or no callus and are considered to be caused by an inadequate biologic environment. A nonunion fracture will not heal without surgical intervention (i.e. bone grafting, rigid fixation).

Multiple factors contribute to delays in fracture healing, including delayed union and nonunion. One cause of delayed fracture healing can be a lack of extraosseous soft tissue, either due to location of the fracture or severe soft tissue damage associated with underlying trauma. A tibial fracture model was created in a population of rats to determine if soft tissue damage significantly affected healing times (23). The study concluded that no detectable difference in fracture healing existed between tibial fractures with and without soft tissue damage, beyond the first three days of healing. In fact, hypervascularization was noticed in the soft tissue trauma group by days seven and 14 (23). The findings of this study confirm that other associated causes for delayed fracture healing in feline tibial fractures exist.

Other factors that can contribute to delayed union or nonunion fracture healing include lack of fracture stability, lack of adequate blood supply, large fracture gaps, interposition of soft tissue between fracture gaps, comminuted fractures, poor nutrition, advanced age, metabolic disturbances, infection, radiotherapy, corticosteroid use, and anticoagulant administration (7, 9, 10, 24, 25). With comminution, it is likely that periosteal stripping and disruption of the soft-

tissue envelope play a significant role in delayed fracture healing. In healthy animals, the periosteum is composed of two layers, an inner osteogenic layer and outer fibrous sleeve (16). The inner layer provides osteogenic cells (precursors for osteoblasts) for growth of the immature skeleton and fracture healing. The outer layer is supportive and carries the vascular and nerve supply to the surface of the cortical bone. Damage to the periosteum could, therefore, result in delayed revascularization of bone early in fracture healing.

MICROVASCULAR PERFUSION TECHNIQUES

Many techniques can be used to describe the microvascular circulation of a tissue substance. The desired vasculature must be injected with a medium that can allow for subsequent vascular visualization and analysis. India ink[a] vascular perfusion is commonly described in human and veterinary literature as a valid infusion medium. The ink coats the vascular bed with a black color, allowing for unobstructed visualization of otherwise indistinguishable blood vessels. Alternate injection media include silicone rubber compounds (Microfil), latex rubber, Micropaque (Barium sulfate suspension in saline), and a gelatin cast. Each of the substances listed must be injected under constant physiologic manual pressure. Microfil polymerizes after injection to form a cast of the selected vascular bed (26). This technique was successfully used in a rabbit femur model as a framework for future microvascular injection studies (26). Latex rubber, when injected at ten pounds per square inch (psi) for 35 seconds (100ml) in a human model, has been shown to result in adequate perfusion (27). Similarly, micropaque injected at 6-7 psi for 5-10 minutes also resulted in adequate perfusion (27). Veins are not filled with microvascular perfusion techniques because fluid run-off is too rapid. Therefore, specimens are adequate representations of the afferent vascular system.

An alternate method to injection of the afferent vascular system is immunohistochemistry. Paraffin-embedded sections of tissue can be stained with a primary antibody (i.e. polyclonal

rabbit, anti-human vWf) against factor VIII/von Willebrand antigens, which are markers for blood vessel endothelium. A secondary antibody (FITC-labeled, anti-murine IgG) is provided to allow for fluorescent detection. Fluorescent intensity can be numerically reported as total pixel intensity, thereby providing a density of the microvascular bed of tissue being evaluated.

SPALTEHOLZ TECHNIQUE

A bone clearing technique is combined with many of the vascular perfusion media chosen, thus allowing for a qualitative or quantitative analysis of the tissue being studied. The Spalteholz bone clearing technique was introduced by Spalteholz in 1911, to provide transparent anatomical specimens for macroscopic evaluation. The final processed specimen is obtained through the methods of fixation, bleaching, dehydration, and embedding. Original technique methods using 10% hydrogen peroxide as a bleaching agent would damage formalin-fixed tissue (28). Surface cell necrosis occurred, resulting in an amber colored specimen. However, when the blood vessels were first treated with a buffered solution, the specimen remained light and transparent for 10 years (unpublished observation) (28). Subsequently, modifications from the original technique have been made by Piechocki (1986), Eitel *et al.* (1986), and Seibold (1990). Steinke (1991) introduced the use of a buffered solution of NaCl, KCl, $CaCl_2$, $MgCl_2$, Na_2CH_3COONa (pH – 7.2) to reduce the damage that was occurring in non-buffered specimens (28).

Methods for the modified Spalteholz technique for bone include decalcification, rinsing, bleaching, dehydration, clearing, and storage. Decalcification is performed by using a buffered solution of hydrochloric acid. Decalcified specimens are then rinsed prior to being bleached. The bleaching process uses either a 10% or 15% dilution of hydrogen peroxide. Dehydration of the specimens is performed by using ethyl alcohol at various dilutions. During this process, the specimens must be kept in an airtight container due to the evaporative properties of ethyl alcohol. In addition, placing tissues under vacuum pressure during this stage and following stages can help

encourage tissues to become transparent and reduces the chances of tissue shrinkage (28). The final clearing stage historically involved the use of benzene and 2-hydroxybenzoic acid methyl ester (methyl salicylate). Because of the carcinogenic dangers of using benzene, alternate chemicals have been substituted. Toluene, a derivative of benzene, is much less toxic and has consequently largely replaced benzene as an aromatic solvent. The final product can be stored in methyl salicylate indefinitely.

CHAPTER III

METHODOLOGY

SPECIMEN COLLECTION

Thirty (30) adult feline and 15 adult canine cadavers were obtained for use in this study. For inclusion in the study, each animal was required to be 1-7 years of age, based on body morphology and dentition when a birthdate was not available. All animals were required to be free of orthopedic disease as evidenced by gross physical examination and available clinical history. All animals were obtained from shelter programs after being euthanized for reasons other than orthopedic disease or the purposes of this study. Dogs selected were required to weigh less than 11.5kg, limiting intramedullary arterial variability that may exist between varying sizes. The right and left pelvic limbs from each cadaver were randomly assigned to one of two groups for gross evaluation using a randomized numerical table. The group labeled A referenced those specimens that were processed first. The group labeled B referenced those processed second. Sixty feline and 30 canine limbs were processed.

SPECIMEN PREPARATION

Each cadaver was placed in dorsal recumbency within a maximum of one hour following euthanasia. The femoral artery and vein in each limb was exposed and the limb prepared as previously described (29-32). The femoral artery and vein were individually isolated and cannulated with an intravenous catheter. The femoral artery was injected with heparinized saline[b]

(approximately 35-50ml for cats, 70ml for dogs) until the venous effluent was visibly clear. India ink was injected under constant manual pressure into the femoral artery (approximately 15-20ml for cats, 35-50ml for dogs) until the ink was visible in the nail beds and/or footpads (Figure 1). Each pelvic limb was disarticulated at the coxofemoral joint and placed in 10% neutral buffered formalin for five days to ensure fixation.

Figure 1. Photograph of a feline pes demonstrating accurate perfusion of the paw with India ink. An incision has been made in the footpad; observe the presence of black ink infiltrating the footpad (arrow).

After fixation, each tibia was harvested by stripping all soft tissue from the surface. The tibiae were sectioned into serial 5.0mm sagittal sections from medial to lateral using a bench top band saw. Although each feline tibia contained approximately 2-3 sections and each canine tibia 3-5 sections, only the central 1-2 sections spanned the entire length of the bone and therefore of adequate length for evaluation. The sectioned tibiae were placed back into formalin until a modified Spalteholz bone clearing technique could be performed (29, 30, 32). This technique produced clear macroscopic specimens, allowing for unobstructed visualization of the injected intramedullary arterial supply (Table 2).

Table 2. Spalteholz Bone Clearing Technique

Decalcification	Buffered solution of 12.5% hydrochloric acid/0.26% disodium ethylenediaminetetraacetic acid (EDTA) dehydrate/water[c]	6 days
Rinse	Running tap water	24 hours
Bleaching	15% hydrogen peroxide[d]	6 days
Dehydration	Ethyl alcohol(EtOH)[e] ,vacuum 50% EtOH 70% EtOH 95% EtOH 100% EtOH	 24 hours 24 hours 48 hours/1 change at 24 hours 72hours/changes at 24 and 48 hrs
Initial Clearing	Toluene[f]	48 hours/1 change at 24 hours
Final Clearing	Methyl salicylate[g]	48 hours/1 change at 24 hours
Storage	Methyl salicylate	Indefinitely

Both tibiae from each cadaver were compared for adequate identification of the intramedullary uptake of India ink. Samples that could not be evaluated due to preparation difficulties (i.e. substrate complications, poor infusion of ink) were discarded. A total of 20 feline limbs and 19 canine limbs remained available for analysis; however, some limbs were from the same animal. In animals where both limbs were adequately perfused (two cats, eight dogs), the limb with the best perfusion was used for statistical evaluation. Using only one limb prevented duplication of results, under our knowledge that there was no significant difference in arterial blood supply between both hindlimbs from the same cadaver. Seventeen feline and 11 canine tibiae were included in the study.

MORPHOMETRIC EVALUATION

Photographic documentation of the sagittal sections was made using a dissecting microscope[h] and SpotSoftware image program[i]. Each bone was placed under 20X magnification, allowing only 8mm of bone to be photographed at one time. The 8mm sections were photographed from distal

to proximal and grouped further into distal, mid-diaphyseal, and proximal sections of bone, with the number of images in each bone section varying depending on bone length. The mean number of images obtained for each bone was 10 (range: 8-12), for cats and dogs. The images were uploaded into the ImageJ[j] morphometric program for further analysis. Each image was converted to gray scale and the window/level was set to automatically adjust to the image. The image threshold was also adjusted, converting the image to black and white. The black pixels were representative of the blood vessels within the medullary canal. The image threshold adjustment was performed manually to appropriately match the blood vessel distribution in the gray scale image. The perimeter of the medullary canal in each image was isolated by drawing a box that extended from each medullar endosteal interface (Figure 2). ImageJ was then utilized to calculate the mean percentage of black pixels within the isolated area, which represented the percentage area occupied by arterial vessels. Three separate analyses of each 8mm image of bone were performed to account for variation in subjective manual adjustment of the threshold for each image.

A. 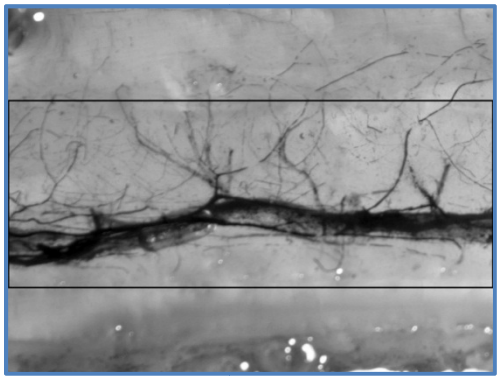 B. 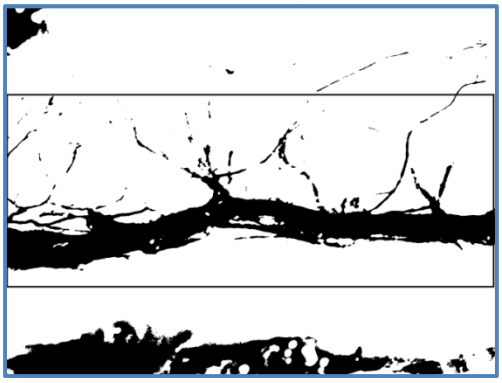

Figure 2. A) Grayscale image representation of an 8mm section of feline tibia at 20X magnification and B) the corresponding adjusted threshold image from which data was subsequently collected. Observe the box that outlines the perimeter of the medullary canal.

Each individual 8mm image was evaluated for the presence of a nutrient artery. The imageJ morphometric program was used to calculate the diameter of the nutrient artery in every image where it was available. Three measurements were obtained in each image if the nutrient artery was present along the entire length of the image. Two measurements were obtained if the nutrient artery was included in half of the image. A measurement was not obtained if only small branching vessels were present. The nutrient artery measurements within each section (distal, mid-diaphyseal, and proximal) were averaged and evaluated for differences between the feline and canine specimens.

STATISTICAL ANALYSIS

All statistical analyses were conducted with PS SAS Version 9.2 (SAS Institute, Cary, NC). Analysis of variances procedures were used to compare species (feline versus canine tibiae) at given bone locations (distal, mid-diaphyseal, and proximal) for significant differences in response variables (intramedullary arterial density and diameter of the nutrient artery). Means with corresponding standard errors are reported. A p-value of less than 0.05 was considered statistically significant for any comparison.

CHAPTER IV

FINDINGS

COLLECTION DATA

Seventeen feline and 11 canine tibiae were analyzed. The right leg was used in seven cats and seven dogs and the left leg used in ten cats and four dogs. The estimated mean age for cats was 2.6 years (1-6years). The estimated mean age for dogs was 2.5 years (1.5-4 years). The mean body weight for cats was 3.87kg (2.87-4.89kg). The mean body weight for dogs was 8.67kg (2.63-9.4kg). Nine male and eight female cats were used. Six male and five female dogs were used. The most common breed of cat included in the study was the domestic shorthaired cat (n = 14). All others were domestic longhaired cats (n = 3). The Chihuahua was the most prevalent dog (n = 3); other breeds included a Chihuahua mix (n = 2), Wire-haired Fox Terrier (n = 2), Rat Terrier (n = 1), mixed breed (n = 2), and Miniature Pinscher (n = 1).

INTRAMEDULLARY ARTERIAL DENSITY

The percentage values obtained for each threshold adjustment performed on each 8mm image were within a mean of 2.8% of one another (range: 0-5%) for both cats and dogs. Mean values and their associated standard error for the intramedullary arterial density in the feline (n = 17) and canine (n = 11) tibiae were 18.281 $\pm$ 2.255% and 21.170 $\pm$ 4.630% (p = 0.384) in the distal section, 22.365 $\pm$ 2.516% and 22.852 $\pm$ 4.286% (p = 0.656) in the mid-diaphyseal section, and 17.132 $\pm$ 1.940% and 20.202 $\pm$ 4.079% (p = 0.366) in the proximal section. Significance was not reached between canine and feline tibiae for each section.

Mean values and their associated standard error for nutrient artery diameter in the feline (distal (n = 13), mid-diaphyseal (n = 16), proximal (n = 13)) and canine (distal (n = 10), mid-diaphyseal (n = 11), and proximal (n = 3)) tibiae were 0.5497 $\pm$ 0.0552mm and 0.2976 $\pm$ 0.0423mm (p = 0.0172) in the distal section, 0.5469 $\pm$ 0.6610mm and 0.3483 $\pm$ 0.0420mm (p = 0.0759) in the mid-diaphyseal section, and 0.6993 $\pm$ 0.0868mm and 0.5982 $\pm$ 0.1064mm (p = 0.5301) in the proximal section. Significance was reached for nutrient artery diameter between feline and canine tibiae in the distal section. Significance was not reached for the mid-diaphyseal or proximal sections.

Subjective evaluation of the specimens revealed a notable difference in the pattern of arterial supply between the canine and feline tibiae. Feline tibiae exhibited one wide nutrient artery with little secondary branching, even as the nutrient artery approached the metaphysis (Figure 3). Alternatively, the canine tibiae exhibited more complex and abundant vascular branching, with a thinner nutrient artery (Figure 4).

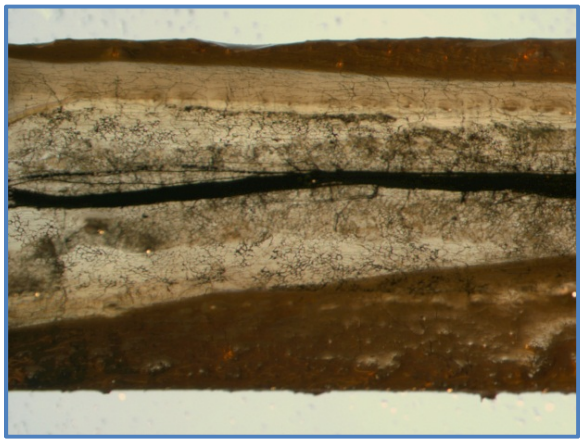

Figure 3. 8mm section of bone representative of the mid-diaphysis from cat I2B. Observe the large diameter of the main nutrient artery and small amount of branching vascularization present.

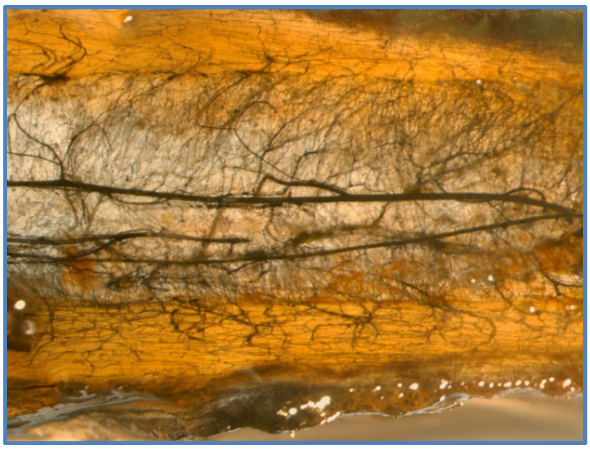

Figure 4. 8mm section of bone representative of the distal diaphysis from canine V3A. Observe the increased amount of vascular branching from the nutrient artery and the smaller nutrient artery size (as compared to that of the cat).

CHAPTER V

DISCUSSION AND CONCLUSIONS

It is well documented that feline tibial fractures have a high rate of delayed union and nonunion complications associated with healing (1, 2, 5, 6). Furthermore, the literature suggests that a lack of adequate arterial supply may account for a large majority of delays in healing (2, 7-9). Despite reports of a high complication rate of delayed union and nonunion feline tibial fractures, a quantitative analysis of the arterial supply of the feline tibia has not been documented. Using previously described methods (29-32), this study determined if either regional or species-related lack of arterial supply is indeed a risk factor for delays in tibial bone healing. Although there was no significant difference found in the intramedullary arterial density between dogs and cats, it should be noted that dogs do have a smaller nutrient artery than cats. This difference in vascular pattern could account for an overall similar intramedullary arterial density while greatly impacting the distribution of blood flow to the cortex. Perhaps, it is the subjectively observed increased arborization within the distal and mid-diaphysis of the canine tibiae that accounts for fewer problems observed in canine tibial fracture healing (Figure 5 and 6).

A. 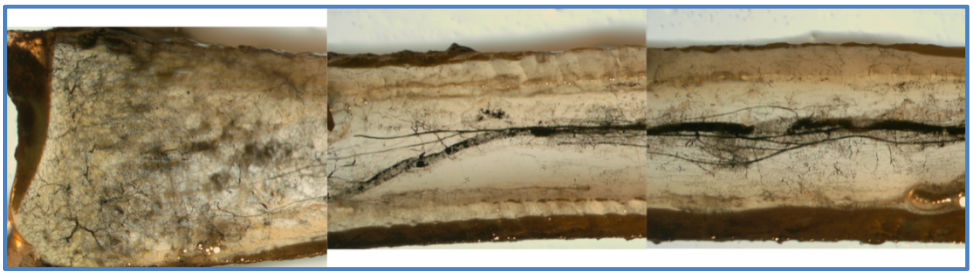

B.

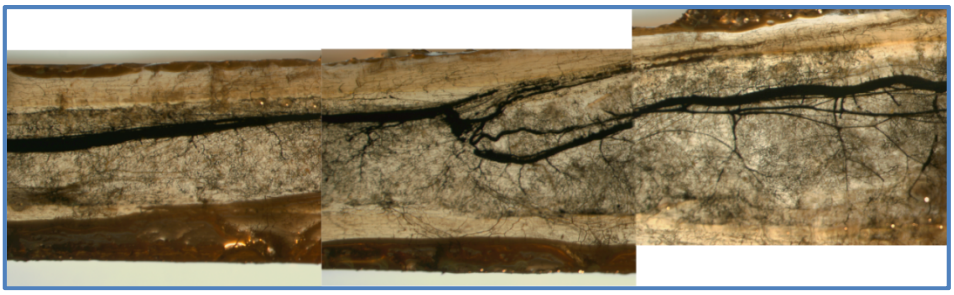

C.

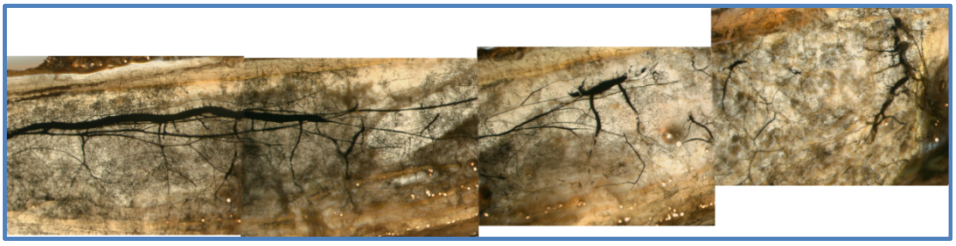

Figure 5. 8mm sections of bone at 20X magnification grouped together to allow for visualization of a representative cat bone (I2B) along its entire length. A) distal section (3 slices), B) mid-diaphysis (3 slices), and C) proximal section (4 slices). Observe the entrance of the nutrient artery in the mid-diaphyseal section of bone.

A.

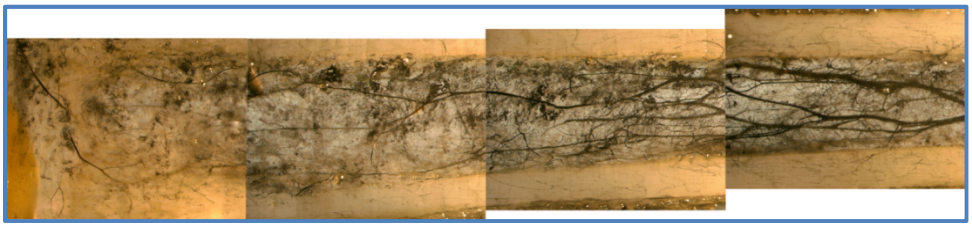

B.

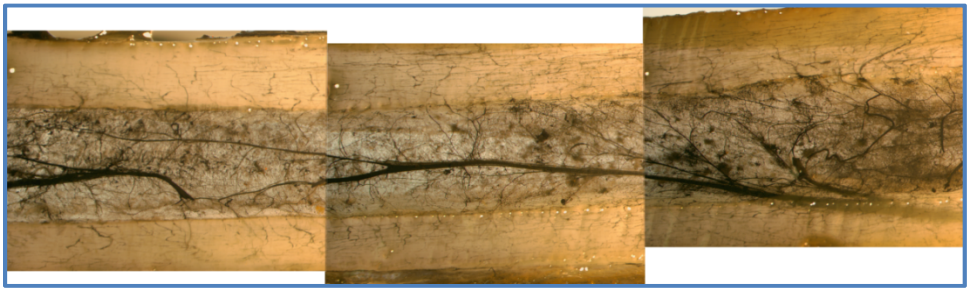

C.

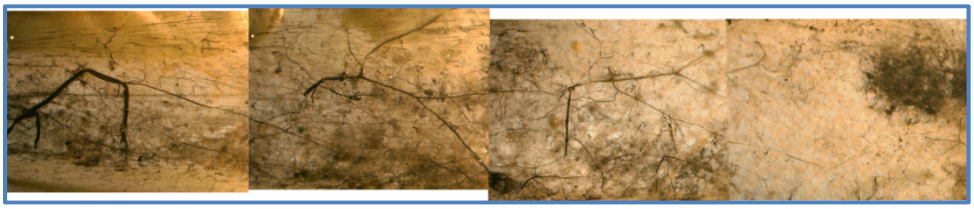

Figure 6. 8mm sections of bone at 20X magnification placed together to allow for visualization of a representative dog bone (V1A). A) distal section (4 slices), B) mid-diaphysis (3 slices), and C) proximal section (4 slices). Observe the entrance of the nutrient artery in the mid-diaphyseal section of bone.

Irrespective of species, mammalian long bones have three sources of arterial supply: proximal and distal metaphyseal arteries, proper nutrient arteries, and periosteal vessels (10, 15, 16). In a healthy cat, the caudal tibial artery, a branch of the popliteal artery, supplies the proper nutrient artery. Upon reaching the medullary canal, the nutrient artery branches proximally and distally, with terminal branches reaching the epiphyseal plate of cartilage and the cortices. Thirty percent of nutrient artery blood flow is responsible for vascularization of the medullary canal; the remaining 70% supplies blood flow to the inner two-thirds of the cortices (16). Periosteal arteries supply the outer one-third of the cortices.

With a disruption of the long bone medullary blood supply following fracture, the periosteal blood supply, via the associated extraosseous soft tissue, provides the major blood supply to the healing bone and callus formation until the endosteal supply is re-established (7, 10, 23, 33). The intact periosteum seals the fracture gap and the periosteal vessels re-vascularize the distal fracture segment. Thus integrity of the periosteum is vital in determining the rate of early healing of a fractured tibia. Damage to overlying soft tissues and periosteum with subsequent loss of periosteal vasculature can result in fracture healing delays in bony union. Therefore, it can be postulated that comminuted fractures will result in greater damage to periosteal vasculature, resulting in an increased incidence of delayed union and nonunion. While this is true, it is also possible that the increase in intramedullary branching observed in the small dogs of this study might result in a faster revascularization of the cortex once the medullary blood supply is re-established. In addition, metaphyseal arteries in healthy animals do not supply a substantial contribution to the afferent vascular system (15), but when the nutrient artery is damaged by

fracture, the metaphyseal arteries hypertrophy and provide a temporary blood supply to metaphyseal cortices. More branching at the metaphysis in dogs, as seen in this study, may therefore offer another explanation for lower rates of nonunion and delayed union in tibial fractures in dogs.

There are obvious limitations of this study. Despite adequate visualization of black ink within the medullary canal, feline and small canine tibiae are very small bones; the mechanics of processing such small specimens can easily result in disruption of the associated vessels. Sagittal sectioning of the bone allowed for only one or two sections of bone to be adequate representations of the entire bone length. This is because sagittal sections cannot be mechanically created to follow the longitudinal path of the nutrient artery. Because the bone is not straight and is triangularly shaped at its proximal end, medullary blood vessels follow the bone contour and are easily cut or destroyed with pure linear sectioning, thereby spuriously reducing the observed percentage of arterial supply within the section of medullary canal. Despite this, all bones were processed with the same technique, thereby standardizing this potential error with all bones, feline and canine.

Many samples were lost to technical error in the beginning of the study due to a lapse in time between euthanasia and injection of India ink. We found that if specimens were injected later than one hour post-euthanasia, perfusion was inadequate, presumably due to intravascular thrombosis. Ideally, animals injected immediately before euthanasia would yield the best perfusion; however, this option was not available to us. It is also important to inject the heparinized saline and India ink under constant manual pressure to yield the best perfusion. This was difficult to do because of the very small catheters (24 gauge) required for feline femoral artery and vein catheterization. The small vessel size may be a limitation to obtaining optimal perfusion within the intramedullary canal. This may be evidenced by some bones exhibiting a blushing effect within the medullary canal, suggestive of a disruption of small arterioles secondary to the pressurized infusion of India ink (Figure 7).

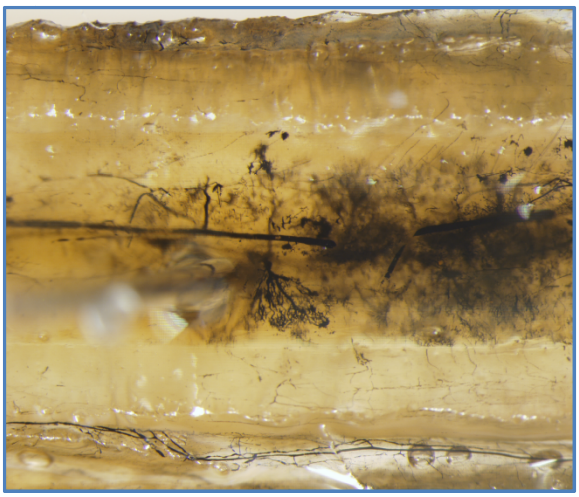

Figure 7. 8mm slice of tibia. Note the blushing effect at the level of the vascular branching from the nutrient artery.

Another limitation of the study lies in recognizing the difficulty in providing objective data. The ImageJ morphometric program provides an excellent way of identifying and calculating the percentage of black in a given area; however, the images contained varying degrees of black pixels within the medullary canal that were present because of individual specimen variation and not representative of blood vessels. Despite strict adherence to a standardized method for performing the Spalteholz technique, all processed samples did not have the same degree of transparency. For example, a more amber-colored bone after processing had darker shades of gray associated with it, which were translated to black when the threshold was adjusted. Our assumption was that all bone images were manually adjusted to the same degree in the ImageJ program, but we attempted to limit any error inherent in the subjective nature of a manual adjustment by evaluating each specimen three consecutive times. An error of 2.8% (range: 0-5%) between consecutive data for each bone image supports the contention that, within the limitations of the software program, the specimens were consistently and uniformly adjusted to the same degree.

Although limitations exist with this method in its ability to delineate the fine detail of branching

arterioles within the bone, the ImageJ method is far more objective than using the human eye to visually compare the obtained images, as has been used in previous morphometric vascular studies (30-34). Although our ability to quantify the intramedullary arterial supply in cats and small dogs was somewhat limited by the technical aspects of the Spalteholz and ImageJ approach we used, other possible avenues such as corrosion casting/scanning electron microscopy or immunohistochemistry methods (35) seemed no more capable of accurately delineating the anatomy of the small branching vessels we observed in feline tibiae. Another alternative would have been to perform microangiography; this method was not available for us to use, but may provide an even better way to evaluate fine arterial supply.

This prospective study provided a quantitative description of the arterial supply of the adult feline tibia, thereby providing some insight to the question of why feline tibial fractures are anecdotally prone to delays in fracture healing. Although it appears the intramedullary arterial density between dogs and cats does not differ in total, thus validating our null hypothesis, the notable difference in the degree of arborization of small arteries and arterioles from the nutrient artery in dogs and cats suggests that the intramedullary arterial supply, as it leaves the nutrient artery and enters the cortex, may be more tenuous in the cat.

REFERENCES

1. Harari J. Treatments for feline long bone fractures. *Vet Clin Small Anim* 2002; 32: 927-947.
2. Nolte DM, Fusco JV, Peterson ME. Incidence of and predisposing factors for nonunion of fractures involving the appendicular skeleton in cats: 18 cases (1998-2002). *J Am Vet Med Assoc* 2005; 226:77-82.
3. Hill FWG. A survey of bone fractures in the cat. *J Small Anim Pract* 1977; 18:457-463.
4. Knecht CD. Fractures in cats: A survey of 100 cases. *Feline Practice* 1978; 8:43-46.
5. Boone EG, Johnson AL, Montavon P, et al. Fractures of the tibial diaphysis in dogs and cats. *J Am Vet Med Assoc* 1986; 188: 41-45.
6. Richardson EF, Thacher CW. Tibial fractures in cats. *Compend Cont Educ* 1993; 15:383-393.
7. DeAngelis MP. Causes of delayed union and nonunion of fractures. *Vet Clin North Am* 1975; 5:251-258.
8. Lu C, Miclau T, Hu D, et al. Ischemia leads to delayed union during fracture healing: A mouse model. *J Orthop Res* 2007; 25:51-61.
9. Schrader SC. Orthopedic surgery. In: The cat: Clinical diseases and clinical management, 2nd edition. Sherding RG (ed). New York: Churchill Livingstone 1994; 1649-1710.
10. Hulse DA, Johnson AL. Fundamentals of orthopedic surgery and fracture management. In: Small Animal Surgery. Fossum TW (ed). St. Louis, Mosby 1997; 705-718, 999-1008.

11. Atilola MAO, Sumner-Smith G. Nonunion fractures in dogs. *Journal of Veterinary Orthopedics* 1984; 3:21-24.
12. Kowalski M, Schemitsch EH, Kregor PJ, et al. Effect of periosteal stripping on cortical bone perfusion: a laser Doppler study in sheep. *Calcif Tissue Int* 1996; 59:24-26.
13. Vaughan LC. A clinical study of non-union fractures in the dog. *J Small Anim Pract* 1964; 5:173-177.
14. Sumner-Smith G, Cawley AJ. Nonunion of fractures in the dog. *J Small Anim Pract* 1970; 11:311-325.
15. Kelly PJ. Anatomy, physiology, and pathology of the blood supply of bones. *Journal of Bone and Joint Surgery* 1968; 50:766-778.
16. Remedios A. Bone and bone healing. *Vet Clin North Am* 1999; 29:1029-1043.
17. Rhinelander FW. Tibial blood supply in relation to fracture healing. *Clin Orthop Relat Res* 1974; 105:34-81.
18. Trueta J. Blood supply and the rate of healing of tibial fractures. *Clin Orthop Relat Res* 1974; 105:11-26.
19. RL Cruess, J. Dumont, C. Newton. Healing of Bone. In: Textbook of Small Animal Orthopaedics. Newton, Nunamaker (eds). Philadelphia. J.B. Lippincott Company. pp. 35-39.
20. Buckwalter JA, Einhorn TA, Bolander ME, et al. Healing of the Musculoskeletal Tissues. In: Fractures in Adults. Rockwood CA, Green DP (Eds). 4th edition. Lippincott, Philadelphia. 1996: 261-276.
21. SE Weisbrode, CE Doige. Bone and Joints. In: Thompson's Special Veterinary Pathology. MD McGavin, WW Carlton, JF Zachary (eds). 3rd edition. Mosby, St. Louis. 2001: 499-508.
22. Cannada LK, Anglen JO, Archdeacon MT, et al. Avoiding complications in the care of fractures of the tibia. AAOS Instructional Course Lectures 2009; 58:27-36.

23. Claes L, Maurer-Klein N, Henke T, et al. Moderate soft tissue trauma delays new bone formation only in the early phase of fracture healing. *Journal of Orthop Res* 2006; 24:1178-1185.
24. Bartels KE. Nonunion. *Vet Clin North Am* 1987; 17:799-809.
25. Hoefle WD. Delayed fracture union, nonunion, and malunion. In: Bojrab's disease mechanisms in small animal surgery. Bojrab MJ. Smeak DD, Bloomberg MS (eds). 2nd ed. Philadelphia. Lea & Febiger. 1993; 689-691.
26. Khan RAA. An anatomical study of the microcirculation in the rabbit femur. *Specialia* 1978; 1101.
27. Crock HV. A revision of the anatomy of the arteries supplying the upper end of the human femur. *J Anat Lond* 1965; 99:77-88.
28. Steinke H, Wolff W. A modified Spalteholz technique with preservation of the histology. *Ann Anat* 2001; 183:91-95.
29. Arnoczky SP, Tarvin GB, Marshall JL. Anterior cruciate ligament placement using patellar tendon. *The Journal of Bone and Joint Surgery* 1982; 64A:217-224.
30. Smith JW, Arnoczky SP, Hersh A. The intraosseous blood supply of the fifth metatarsal: Implications for proximal fracture healing. *Foot & Ankle* 1992; 13:143-152.
31. Welch JA, Boudrieau RJ, DeJardin LM, et al. The intraosseous blood supply of the canine radius: Implications for healing of distal fractures in small dogs. *Vet Surg* 1997; 26:57-61.
32. Boudrieau RJ, Kaderly RE, Arnoczky SP, et al. Vascularized patellar tendon graft technique for cranial cruciate ligament substitution in the dog – vascular evaluation. *Vet Surg* 1985; 14:196-203.
33. Macnab I, deHaas WG. The role of periosteal blood supply in the healing of fractures of the tibia. *Clin Orthop* 1974; 105:27-33.

34. Mikic Z. Blood supply of the articular disc of the antebrachiocarpal joint in dogs. *J Anat* 1992; 181: 447-453.

35. Hayashi K, Bhandal J, Kim SY, et al. Immunohistochemical and histomorphometric evaluation of vascular distribution in intact canine cranial cruciate ligament. *Vet Surg* 2010; 40:192-197.

APPPENDIX

FOOTNOTES

a. India ink, waterproof. Item number 44204. Chartpak, Inc., Leeds, MA 01053. USA.

b. Heparinized saline. 3mL of 1:1,000 heparin added to 1L of 0.9% sodium chloride.

c. RDF 12.5% (v/v) hydrochloric acid, 0.26% (w/v) disodium EDTA dehydrate, water. Item number D1210-1. StatLab. McKinney, TX, 75071. USA.

d. Hydrogen peroxide solution, 30% (w/w) water. Item number H1009. Sigma-Aldrich, St. Louis, MO, 63103. USA. Diluted in distilled water.

e. Ethyl alcohol 200 proof, absolute, anhydrous ACS. Item number 111000200. Pharmco Products, Inc. Shelbyville, KY, 40065. USA.

f. Toluene $\geq$ 99.5%, ACS reagent. Item number 179418. Sigma-Aldrich. St. Louis, MO, 63103. USA.

g. 2-hydroxybenzoic acid methyl ester (methyl salicylate). Item number M6752. Sigma-Aldrich. St. Louis, MO, 63103. USA.

h. Olympus SZX7 dissecting microscope. Model number SZX-1LLD2-100. Hayagaya, Shibuya-ku, Tokyo, Japan.

i. SpotSoftware. v. 4.5 Diagnostic Instruments, Inc. Sterling Heights, MI, 48314. USA.

j. ImageJ Image Processing and Analysis in Java. v. 1.43. http://rsb.info.nih.gov/ij/

VITA

Danielle Renee Dugat, DVM

Candidate for the Degree of

Master of Science

Thesis: QUANTITATIVE ANALYSIS OF THE INTRAMEDULLARY ARTERIAL SUPPLY OF THE FELINE TIBIA; IS THERE A CAUSAL RELATIONSHIP TO DELAYED AND NONUNION FRACTURE HEALING?

Major Field: Veterinary Biomedical Sciences

Biographical:

Education:

Completed the requirements for the Master of Science in Veterinary Biomedical Sciences at Oklahoma State University, Stillwater, Oklahoma in May, 2011.

Completed the requirements for the Doctor of Veterinary Medicine at Oklahoma State University, Stillwater, Oklahoma in May, 2007.

Completed the requirements for the Bachelor of Science in Animal Science/Pre-veterinary option at California State Polytechnic University, Pomona, California in June, 2003.

Experience:

Residency, Small Animal Surgery. Oklahoma State University, Veterinary Clinical Sciences Stillwater, Oklahoma. Will be completed in July, 2011.

Internship, Small Animal Medicine and Surgery. Oklahoma State University, Veterinary Clinical Sciences, Stillwater, Oklahoma. Completed in June, 2008.

Professional Memberships:

Phi Kappa Phi Honor Society – Membership offered in February, 2011
Phi Zeta Veterinary Honor Society, Nu Chapter – Inducted in March, 2010
Gamma Sigma Delta Honor Society – Inducted in March, 2002
Alpha Lambda Delta Honor Society – Inducted in January, 2001

Name: Danielle Renee Dugat Date of Degree: May, 2011

Institution: Oklahoma State University Location: Stillwater, Oklahoma

Title of Study: QUANTITATIVE ANALYSIS OF THE INTRAMEDULLARY ARTERIAL SUPPLY OF THE FELINE TIBIA; IS THERE A CAUSAL RELATIONSHIP TO DELAYED AND NONUNION FRACTURE HEALING?

Pages in Study: 31 Candidate for the Degree of Master of Science

Major Field: Veterinary Biomedical Sciences

Scope and Method of Study:

Clinical observations suggest that feline tibial fractures are prone to delayed union and nonunion healing complications. This study sought to quantitatively describe the intramedullary arterial supply of the adult feline tibia and determine if the arterial supply is different from that of adult small dogs, who seemingly do not exhibit the same rates of delayed and nonunion fracture healing. Our null hypothesis was that the intramedullary arterial density and diameter of the nutrient artery in the adult feline tibia was the same as the age and size matched dog. Using microvascular injection and modified Spalteholz techniques, cadaveric feline and canine pelvic limbs were prepared to characterize the intramedullary arterial supply of the tibia. Processed specimens were evaluated using the ImageJ morphometric program. Statistical comparisons were made between cats and dogs for the intramedullary arterial density and diameter of the nutrient artery.

Findings and Conclusions:

There was no significant difference in the intramedullary arterial density between dog and cat tibiae. The feline nutrient artery diameter (0.5497 ± 0.0552mm) was significantly different than the canine nutrient artery (0.2976 ± 0.0423mm) in the distal section of bone. Dogs subjectively exhibited more branching vessels in the distal and mid-diaphyseal bone sections. Delayed fracture healing in the feline tibia does not appear to be due to diminished intramedullary arterial supply. However, a lack of diffuse arborization of the arterial supply to the cortex of the mid-diaphyseal and distal feline tibia may explain, in part, why feline tibial delayed or nonunions may be more common than those in dogs.

ADVISER'S APPROVAL: Mark C. Rochat, DVM, MS, DACVS